

Lagrangian stochastic modelling for oil spills turbulent dispersion on ocean surface

Gianni Pagnini¹, Susanna Strada², Alberto Maurizi³, Francesco Tampieri³

¹*CRS4, Polaris Bldg. 1, I-09010 Pula (CA), Italy*
pagnini@crs4.it

²*CNRS-Laboratoire d'Aérodynamique, University of Toulouse, Toulouse, France*
susanna.strada@aero.obs-mip.fr

³*ISAC-CNR, via Gobetti 101, I-40129 Bologna, Italy*
a.maurizi@isac.cnr.it
f.tampieri@isac.cnr.it

Communicated by Nicola Bellomo

Abstract

Releases of liquid petroleum hydrocarbon into the environment, especially into the ocean, are called *oil spills*. To correctly model dispersion on ocean surface both large and small scale processes must be considered. In fact, the motion of the centre of mass is driven by large scale meandering and spot enlarging is controlled by small scale turbulence. A Lagrangian stochastic model for turbulent dispersion of oil spills on ocean surface is here formulated: large scale meandering is analytically prescribed by the stream function proposed by Bower for meandering jet in the Gulf Stream; small scale turbulence has been modelled by a Lagrangian stochastic process for turbulent relative dispersion which is based on turbulent flow rotation. Numerical simulations are performed to highlight the effects on oil spills dispersion of differences in the velocity field intensity and those due to releases in the centre or in the boundary of a meandering jet.

Keywords: Lagrangian stochastic model, turbulent dispersion, oil spills.

AMS Subject Classification: 60J60, 76F25, 86A05

1. Introduction.

The name *oil spills* is referred to releases of liquid petroleum hydrocarbon into the environment, mainly due to human activity, which clearly embodies a form of pollution. This term often is used for marine oil spills, when oil is released into the ocean or coastal waters, and it may be a variety of materials including crude oil, refined petroleum products (gasoline or diesel fuel), oily refuse or oil mixed in waste. To reduce the negative effects

Received 2010 01 19, in final form 2010 06 12

Published 2010 06 21

of these releases, besides prevention techniques [1], prediction models are of paramount importance especially to improve human response on land to minimize the consequences.

In open seas, oil spills damage the organisms that reach the water surface to breath, birds that seek for food in the water and also micro-organisms that live in the surface, while they damage flora and fauna in the coastal areas. Moreover, the oil percolation in the beach creates sedimentation that makes hard the land reclamation. Obviously, environmental damages due to oil spills have dangerous effects also on human health and they are a problem for social, economical and touristic reasons.

Lagrangian stochastic modelling has been largely validated for turbulent dispersion in several applied problems included environmental, see for example Ref. [2] for the atmosphere and Ref. [3] for the ocean. Here a Lagrangian stochastic model is developed to study the dispersion of oil spills on the ocean surface. This model includes both large and small scale processes. In particular, the meandering due to large scale is modelled considering for the centre of mass motion the analytical stream function proposed by Bower for the Gulf Stream meandering jet [4], and the enlarging of the oil spot, which is driven by small scale turbulence, is studied by a Lagrangian stochastic model for turbulent relative dispersion [5] when particle pair motion is correlated and by the sum of the stream meandering and an Ornstein–Uhlenbeck stochastic process when particles become statistically independent.

The rest of the paper is organized as follows. In Section 2 the main characteristics of ocean turbulence are reminded. In Section 3 the dispersion model is developed and in Section 4 numerical simulations are performed. In Section 5 conclusions are given and further development addressed.

2. Turbulence in the ocean surface.

In order to define the physical framework under consideration, some characteristics of turbulence in the ocean are reminded; the interest reader can find more details in Refs. [6,7]. For what concern tracers dispersion on the ocean surface, the most important layer is the Upper Mixed Layer (UML). Here temperature is constant and its depth is around 100 m, at the tropics, while at high latitudes it ranges between $10 \div 20$ m in the summer and several hundreds of meters in the winter. Velocity fluctuations are of the order 1 cm s^{-1} and rapidly decrease when the depth increases. The bottom boundary layer of UML is characterized by an irregular shape due to internal waves and large scale turbulent vortexes, with dimension comparable with the depth of the UML itself. In general, at all latitudes, the

density increases with the depth, as well as the saltiness, even if a different vertical profile characterizes each geographical area.

Turbulence is generated mainly by overturning of surface waves, convection in layer with unstable stratification and by a number of instabilities, e.g. instability of local velocity gradient in internal waves, instability of vertical velocity gradient in oceanic large scale stratified flows.

The horizontal dimension of the ocean can be assumed as the larger length scale L_{max} , and the smallest length scale L_{min} can be estimated by Kolmogorov theory of local isotropic turbulence [8], i.e. $L_{min} = \eta = (\nu^3/\varepsilon)^{1/4}$, where ν is the kinematic viscosity and ε is the mean rate of turbulent kinetic energy dissipation. A good estimation of ε is $10^{-1} \div 10^{-5} \text{ cm}^2 \text{ s}^{-3}$ and then, since in the ocean $\nu \simeq 10^{-2} \text{ cm}^2 \text{ s}^{-1}$, L_{min} ranges between 1 mm and 1 cm. For what concern temporal scales, also in this case from Kolmogorov theory the shortest timescale follows to be $T_{min} = \tau_\eta = (\nu/\varepsilon)^{1/2}$ and for the same value of ε considered above it follows that $T_{min} = 1 \div 100 \text{ s}$. Much more difficult is to establish the longer timescale T_{max} because the timescale of large lengthscale motions is not fixed. Temporal cycles are of some years but they depend also on climate changes whose characteristic time is of the order of geological eras. However, when turbulence is considered, it can be assumed $T_{max} = 3 \cdot 10^7 \text{ s}$.

When the horizontal dimensions of turbulent motion are much more larger than the lengthscale of buoyancy or the depth of the UML, then large scale turbulence occurs and the vorticity axis is approximately vertical. In general, such macro turbulence can be generated by circular motion due to several mechanisms: turbulent wind field, barotropic or baroclinic instabilities, vortexes generated by topography of the ocean bottom, etc... One of the main large scale manifestation of turbulence in the ocean are synoptic vortexes, which have dimension around 100 km.

3. Oil spill dispersion model.

3.1. Lagrangian stochastic model formulation

Oil spills need months, or even years, to clean up and this depends on several elements. Moreover, since this cleaning process is slow in time and, up to special circumstances, it involves a small fraction of the total volume of oil released then oil spills can be considered non-reacting passive tracers.

Turbulent dispersion in the ocean is given by the combination of large scale turbulence, which is responsible of the motion of the centre of mass, with small scale turbulence, which drives the enlarging of the oil spot. In particular the enlarging of the oil spill is a problem of turbulent relative dispersion.

Lagrangian stochastic models have been largely used and validated in problems of turbulent dispersion both in atmosphere and ocean [2,3,5,9–13]. Let $(\mathbf{x}^{(1)}, \mathbf{x}^{(2)})$ and $(\mathbf{u}^{(1)}, \mathbf{u}^{(2)})$ be the position and the velocity of two particles, respectively, and let $\Delta\mathbf{x}$ and $\Delta\mathbf{u}$ be the relative position and the relative velocity, and $\Sigma\mathbf{x}$ and $\Sigma\mathbf{u}$ be the double of centre of mass position and velocity, then

$$(1) \quad \begin{cases} \Sigma\mathbf{x} = \mathbf{x}^{(1)} + \mathbf{x}^{(2)} \\ \Sigma\mathbf{u} = \mathbf{u}^{(1)} + \mathbf{u}^{(2)} \end{cases}, \quad \begin{cases} \Delta\mathbf{x} = \mathbf{x}^{(1)} - \mathbf{x}^{(2)} \\ \Delta\mathbf{u} = \mathbf{u}^{(1)} - \mathbf{u}^{(2)} \end{cases},$$

and for each particle

$$(2) \quad \begin{cases} \mathbf{x}^{(1)} = \Sigma\mathbf{x} - \frac{\Delta\mathbf{x}}{2} \\ \mathbf{u}^{(1)} = \Sigma\mathbf{u} - \frac{\Delta\mathbf{u}}{2} \end{cases}, \quad \begin{cases} \mathbf{x}^{(2)} = \Sigma\mathbf{x} + \frac{\Delta\mathbf{x}}{2} \\ \mathbf{u}^{(2)} = \Sigma\mathbf{u} + \frac{\Delta\mathbf{u}}{2} \end{cases}.$$

The motion of the centre of mass of each particle pair is deterministically described by the integral equation

$$(3) \quad \Sigma\mathbf{x}(t) = \Sigma\mathbf{x}(0) + \int_0^t \mathbf{U}(\Sigma\mathbf{x}, \tau) d\tau,$$

where $\mathbf{U}(\Sigma\mathbf{x}, t)$ is the average velocity field in the place $\Sigma\mathbf{x}$ at time t and it can be determined by using an oceanic circulation model or introducing an analytical stream function. Here the second approach is followed and the stream function proposed by A.S. Bower [4] to reproduce meandering jet of the Gulf Stream is adopted.

The enlarging of the oil spill is described by relative dispersion of particle pairs. When the modulus of particle separation $|\Delta\mathbf{x}| = \Delta x = (\Delta\mathbf{x} \cdot \Delta\mathbf{x})^{1/2}$ is less than the Eulerian lengthscale λ the particle motion is correlated and a turbulent relative dispersion model has to be used. When r is larger than λ , particles become statistically independent and the motion of each one $\mathbf{x}^{(i)}$ follows from the sum of the large scale average velocity field \mathbf{U} and a turbulent fluctuation \mathbf{u}'

$$(4) \quad \mathbf{x}(t) = \mathbf{x}(0) + \int_0^t (\mathbf{U}(\mathbf{x}, \tau) + \mathbf{u}'(\mathbf{x}, \tau)) d\tau.$$

For absolute dispersion of independent particles, the evolution of the turbulent velocity fluctuation \mathbf{u}' can be modelled by an Ornstein–Uhlenbeck stochastic process

$$(5) \quad d\mathbf{u}' = -\frac{\mathbf{u}'}{\tau_L} dt + \sqrt{C_0\varepsilon} d\mathbf{W},$$

where $d\mathbf{W}$ is a Wiener process with zero mean and variance dt , the noise amplitude $\sqrt{2C_0\varepsilon}$ is chosen consistently with the second order Lagrangian

structure function, i.e. $S_L = \langle (u_i^{(j)}(0) - u_i^{(j)}(t))^2 \rangle = C_0 \varepsilon t$, $j = 1, 2$, $i = 1, 2, 3$, where C_0 is a universal constant, and τ_L is the Lagrangian integral timescale defined by

$$(6) \quad \tau_L = \frac{2\sigma^2}{C_0\varepsilon},$$

with $\sigma^2 = \langle \mathbf{u}' \cdot \mathbf{u}' \rangle / 3$. When $t \ll \tau_L$, or $t \gg \tau_L$, the dispersive regime is called inertial, or diffusive.

It is important to remark that if the scale of the average velocity gradient is less than the Eulerian lengthscale λ then when $r < \lambda$ the field \mathbf{U} can be considered approximately constant and particle relative motion does not depend on \mathbf{U} . In this case relative dispersion can be modelled in homogeneous, stationary and isotropic turbulence and here the Lagrangian stochastic process introduced in Ref. [5] is chosen.

3.2. Stream function

The stream function adopted in the present model is that proposed by A.S. Bower [4] to study the meandering jet of the Gulf Stream. In the present analysis the steady state $t = 0$ is considered and then it reads

$$(7) \quad \psi(x, y) = \psi_0 \left(1 - \tanh \left[\frac{y - A \cos(\mathcal{K}x)}{\Lambda \sqrt{1 + k^2 A^2 \sin^2(\mathcal{K}x)}} \right] \right),$$

where x and y are the coordinates in an fixed inertial system, $\Lambda = 40$ km is the semi-amplitude of the jet, ψ_0 is a scale factor to determine the maximum velocity as $s_c = \psi_0/\Lambda$, $A = 50$ km is the amplitude of the wave packet, $\mathcal{K} = 2\pi/L$ is the wave number associated to the wave length of the meander $L = 400$ Km.

The two-dimension components of the average velocity field $\mathbf{U} = (U, V)$ are given by $U = -\partial\psi/\partial y$ and $V = \partial\psi/\partial x$.

3.3. Lagrangian stochastic model for turbulent relative dispersion

For separation less than the Eulerian lengthscale λ , the enlarging of the oil spot is driven by small scale turbulence and homogeneity, stationarity and isotropy are assumed. With this modelling assumption the Lagrangian stochastic model for turbulent relative dispersion formulated in Ref. [5] can be chosen and in this section it is briefly reminded. To lighten notation, let $\Delta\mathbf{x}$ and $\Delta\mathbf{u}'$ be replaced by \mathbf{r} and \mathbf{u} , respectively. The relative motion between two fluid particles is described by the stochastic differential equations

$$(8) \quad d\mathbf{r} = \mathbf{u} dt, \quad d\mathbf{u} = \mathbf{a} dt + \sqrt{2C_0\varepsilon} d\mathbf{W},$$

where $\mathbf{a} = \mathbf{a}(\mathbf{u}, \mathbf{r}, t)$ is a nonlinear drift term and the phase-space Lagrangian probability density function (PDF) $p_L(\mathbf{u}, \mathbf{r}; t|\mathbf{r}_0)$ evolves according to the Fokker–Planck equation

$$(9) \quad \frac{\partial p_L}{\partial t} = -\frac{\partial}{\partial r_i}(u_i p_L) - \frac{\partial}{\partial u_i}(a_i p_L) + C_0 \varepsilon \frac{\partial^2 p_L}{\partial u_i \partial u_i}.$$

The model is constructed in the framework of the Well-Mixed Condition [9], which guarantees consistency between Eulerian and Lagrangian statistics, and then, after applied the integral relation $p_E(\mathbf{u}, \mathbf{r}, t) = \int p_L(\mathbf{u}, \mathbf{r}; t|\mathbf{r}_0) d\mathbf{r}_0$ to (9), the drift term is determined as

$$(10) \quad a_i p_E = C_0 \varepsilon \frac{\partial p_E}{\partial u_i} + \Phi_i, \quad \frac{\partial \Phi_i}{\partial u_i} = -\frac{\partial p_E}{\partial t} - \frac{\partial u_i p_E}{\partial r_i},$$

where p_E is the Eulerian PDF of turbulent velocity fluctuation and $|\Phi| \rightarrow 0$ when $|\mathbf{u}| \rightarrow \infty$. However, for a given Eulerian PDF, the drift coefficient \mathbf{a} defined in (10) is determined up to an additive term with zero divergence with respect to \mathbf{u} . The closure derived in [5] is based on the physical picture of fluid particle pair as a couple of material points rotating around their centre of mass. In this case, exact kinematic results can be obtained and used to uniquely determine the drift term $\mathbf{a}(\mathbf{u}, \mathbf{r}, t)$ in (8). In fact, the Lagrangian relative velocity can be written as

$$(11) \quad \mathbf{u} = u_{\parallel} \frac{\mathbf{r}}{r} + \boldsymbol{\Omega} \times \mathbf{r},$$

where $\boldsymbol{\Omega}$ is a pair angular velocity defined as

$$(12) \quad \boldsymbol{\Omega} = \frac{1}{r^2}(\mathbf{r} \times \mathbf{u}).$$

The Lagrangian relative acceleration is defined as $\mathbf{A} = d\mathbf{u}/dt = \mathbf{A}^{(1)} - \mathbf{A}^{(2)}$ where $\mathbf{A}^{(i)} = d\mathbf{u}^{(i)}/dt$, and its most general form, when (11) holds, is

$$(13) \quad \mathbf{A} = \alpha_1 \frac{\mathbf{r}}{r} + \alpha_2(\boldsymbol{\Omega} \times \mathbf{r}) + \alpha_3(\mathbf{r} \times (\boldsymbol{\Omega} \times \mathbf{r})),$$

that, using (12), can be rearranged as

$$(14) \quad \mathbf{A} = (\alpha_1 - \alpha_2 u_{\parallel}) \frac{\mathbf{r}}{r} + \alpha_2 \mathbf{u} + \alpha_3 r^2 \boldsymbol{\Omega},$$

where α_1 , α_2 and α_3 are coefficients to be determined by symmetries and properties of the process by relating the exact kinematic formula (14) to the drift term of the stochastic model (8).

The isotropy permits to move to spherical reference frame: $\{\mathbf{u}\} \rightarrow \{u_{\parallel}, u_{\perp}, \alpha\}$ where $u_{\parallel} = \mathbf{u} \cdot \mathbf{r}/r$, $u_{\perp}^2 = u^2 - u_{\parallel}^2$, $u^2 = \mathbf{u} \cdot \mathbf{u}$, and $\alpha \in [0; 2\pi]$ is a uniformly distributed angle. In the new reference frame (8) becomes

$$(15) \quad dr = u_{\parallel} dt, \quad du_{\parallel} = \chi_{\parallel} dt + \sqrt{2C_0\varepsilon} dW_{\parallel}, \quad du_{\perp} = \chi_{\perp} dt + \sqrt{2C_0\varepsilon} dW_{\perp}.$$

As pointed out by [12], in isotropic turbulence the drift term \mathbf{a} in Cartesian coordinates has the following general form

$$(16) \quad \mathbf{a}(u_{\parallel}, u_{\perp}, r, t) = \varphi(u_{\parallel}, u_{\perp}, r, t) \frac{\mathbf{r}}{r} + \psi(u_{\parallel}, u_{\perp}, r, t) \frac{\mathbf{u}}{u},$$

where φ and ψ are two unknown scalar functions. The drift terms in Cartesian and spherical coordinates are related to each other as follows [14]

$$(17) \quad \chi_{\parallel}(u_{\parallel}, u_{\perp}, r, t) = a_{\parallel} + \frac{u_{\perp}^2}{r} = \varphi + \psi \frac{u_{\parallel}}{u} + \frac{u_{\perp}^2}{r},$$

$$(18) \quad \chi_{\perp}(u_{\parallel}, u_{\perp}, r, t) = \frac{u_{\perp} a_{\perp} - u_{\parallel} a_{\parallel}}{u_{\perp}} - \frac{u_{\parallel} u_{\perp}}{r} + \frac{C_0\varepsilon}{u_{\perp}} = \psi \frac{u_{\perp}}{u} - \frac{u_{\parallel} u_{\perp}}{r} + \frac{C_0\varepsilon}{u_{\perp}}.$$

From (17) and (18) the following expressions for φ and ψ are found

$$(19) \quad \varphi = \chi_{\parallel} - \frac{u_{\parallel}}{u_{\perp}} \chi_{\perp} - \frac{u^2}{r} + \frac{u_{\parallel}}{u_{\perp}} \frac{C_0\varepsilon}{u_{\perp}},$$

$$(20) \quad \psi = \frac{u}{u_{\perp}} \chi_{\perp} + \frac{uu_{\parallel}}{r} - \frac{u}{u_{\perp}} \frac{C_0\varepsilon}{u_{\perp}},$$

that substituted in (16) yields

$$(21) \quad \mathbf{a} = \chi_{\parallel} \frac{\mathbf{r}}{r} + \frac{1}{u_{\perp}} \left(\mathbf{u} - u_{\parallel} \frac{\mathbf{r}}{r} \right) \left(\chi_{\perp} - \frac{C_0\varepsilon}{u_{\perp}} \right) + \boldsymbol{\Omega} \times \mathbf{u}.$$

For the noise $d\mathbf{W}$, a representation of the type of (16) cannot be given because a Markovian noise is not a function of \mathbf{r} or \mathbf{u} . However, keeping in mind that in the chosen reference frame the motion is only radial with respect to the centre of mass, the noise can be explicitly considered in the longitudinal direction while in the transverse direction it is implicitly taken into account by the dependence of the drift term on the stochastic variable u_{\perp} , finally

$$(22) \quad d\mathbf{W} = \left(d\mathbf{W} \cdot \frac{\mathbf{r}}{r} \right) \frac{\mathbf{r}}{r} = dW_{\parallel} \frac{\mathbf{r}}{r}.$$

Hence, considering that

$$(23) \quad \mathbf{A} dt = \mathbf{a} dt + \sqrt{2C_0\varepsilon} d\mathbf{W}$$

formally holds, substitution of (16) and (22) in (23) gives

$$(24) \quad \mathbf{A} dt = \left(\varphi dt + \sqrt{2C_0\varepsilon} dW_{\parallel} \right) \frac{\mathbf{r}}{r} + \psi \frac{\mathbf{u}}{u} dt.$$

Now, comparing (24) and (14) the coefficients α_2 and α_3 are determined as $\alpha_2 = \psi/u$ and $\alpha_3 = 0$. Furthermore, the above definition of A_{\parallel} gives

$$\alpha_1 dt = A_{\parallel} dt = a_{\parallel} dt + \sqrt{2C_0\varepsilon} dW_{\parallel},$$

so that α_1 includes all the effects of the stochastic noise. From comparison of (24) and (14) the following equation is obtained for φ

$$(25) \quad \varphi = a_{\parallel} - \alpha_2 u_{\parallel}.$$

Substitution in (25) of φ by (19) and of a_{\parallel} by (17) gives

$$(26) \quad \frac{u_{\parallel}}{u_{\perp}} \left(\chi_{\perp} - \frac{C_0\varepsilon}{u_{\perp}} \right) + \frac{u^2}{r} = \frac{u_{\perp}^2}{r} + \alpha_2 u_{\parallel}.$$

From (22) and arguments above it, the effects of the stochastic noise are only along the \mathbf{r}/r direction. Therefore α_2 appears to be independent of $C_0\varepsilon$ because it is the coefficient in the $(\boldsymbol{\Omega} \times \mathbf{r})/|\boldsymbol{\Omega} \times \mathbf{r}|$ direction. This means that $\chi_{\perp} = C_0\varepsilon/u_{\perp} + f(u_{\parallel}, u_{\perp}, r)$. The system of stochastic equations (15) gives the evolution in time of the PDF $p_L(u_{\parallel}, u_{\perp}, r; t|r_0)$ that can be composed by the product $p_L(u_{\parallel}, r; t|u_{\perp}, r_0)p(u_{\perp}; t|r_0)$ and from this, in stationary turbulence, it is statistically sound to have $\chi_{\perp} = \chi_{\perp}(u_{\perp}, r)$. From dimensional analysis χ_{\perp} assumes the form

$$\chi_{\perp} = \frac{C_0\varepsilon}{u_{\perp}} + k \frac{u_{\perp}^2}{r},$$

where k is a dimensionless real number which has to be determined. However, for numerical stability k must be zero [5] and χ_{\perp} is given by

$$(27) \quad \chi_{\perp} = \frac{C_0\varepsilon}{u_{\perp}},$$

therefore $\alpha_2 = u_{\parallel}/r$. Finally, with $\alpha_1 = A_{\parallel}$, $\alpha_2 = u_{\parallel}/r$, $\alpha_3 = 0$, formula (13) becomes

$$(28) \quad \mathbf{A} = \left(A_{\parallel} + \frac{u_{\perp}^2}{r} \right) \frac{\mathbf{r}}{r} + \boldsymbol{\Omega} \times \mathbf{u}.$$

Note that, since (28) is recovered using (21) and (27) it follows from combination of exact kinematic results and the stochastic model.

The physical picture described above selects a unique model in the Well-Mixed class, and thereby solves the drift indeterminacy. In fact, applying the Well-Mixed Condition to (15) and using (27), the following Fokker-Planck equation is obtained

$$(29) \quad \frac{\partial p_E}{\partial t} + \frac{1}{r^2} \frac{\partial}{\partial r} (r^2 u_{\parallel} p_E) + \frac{\partial}{\partial u_{\parallel}} (\chi_{\parallel} p_E) = C_0 \varepsilon \left[\frac{\partial^2 p_E}{\partial u_{\parallel}^2} + \frac{1}{u_{\perp}} \frac{\partial}{\partial u_{\perp}} \left(u_{\perp} \frac{\partial p_E}{\partial u_{\perp}} \right) \right],$$

with the normalization condition $2\pi \int_{-\infty}^{+\infty} du_{\parallel} \int_0^{+\infty} du_{\perp} u_{\perp} p_E(u_{\parallel}, u_{\perp}; t|r) = 1$. Integrating (29) in $u_{\parallel} \in]-\infty; u_{\parallel}]$, the parallel drift term χ_{\parallel} is determined by

$$(30) \quad \chi_{\parallel} = C_0 \varepsilon \frac{1}{p_E} \frac{\partial p_E}{\partial u_{\parallel}} - \frac{1}{p_E} \Psi(u_{\parallel}, u_{\perp}, r, t),$$

where

$$(31) \quad \Psi = \int_{-\infty}^{u_{\parallel}} \left\{ \frac{\partial p_E}{\partial t} + \frac{1}{r^2} \frac{\partial}{\partial r} (r^2 u'_{\parallel} p_E) - \frac{C_0 \varepsilon}{u_{\perp}} \frac{\partial}{\partial u_{\perp}} \left(u_{\perp} \frac{\partial p_E}{\partial u_{\perp}} \right) \right\} du'_{\parallel},$$

with the general assumptions

$$\chi_{\parallel} p_E \rightarrow 0, \quad \frac{\partial p_E}{\partial u_{\parallel}} \rightarrow 0, \quad |u_{\parallel}| \rightarrow \infty.$$

Equation (30) shows the dependence of the longitudinal drift χ_{\parallel} on u_{\perp} , which is different from Quasi-One-Dimensional models, e.g. [12,13].

In order to define an operational model a Eulerian PDF p_E is needed. However, noting that by (27) the drift term a_i (16) becomes

$$(32) \quad a_i = \varphi \frac{r_i}{r} + \frac{u_{\parallel} u_i}{r},$$

the choice of p_E reduces to the choice of φ . The choice studied in Ref. [5] and adopted here is

$$(33) \quad \varphi = -\frac{u_{\parallel}}{\tau(r)} + \gamma \frac{u_{\parallel}^2}{r} + \frac{1}{2} \frac{u_{\perp}^2}{r} + \rho \frac{u_{\parallel} u_{\perp}}{r},$$

where $\{\gamma, \rho\}$ are the model parameters, which will be determined by imposing Eulerian statistics. Obviously, the choice of φ does not guarantee

the existence of p_E and then the fulfillment of the Well-Mixed Condition. The relaxation-time, denoted by $\tau(r)$, depends on the particle separation and is defined as

$$(34) \quad \tau(r) = \frac{\langle u_{\parallel}^2 \rangle}{C_0 \varepsilon},$$

where $\langle u_{\parallel}^2 \rangle$ is the Eulerian second order structure function such that

$$(35) \quad \langle u_{\parallel}^2 \rangle = \begin{cases} C_K (\varepsilon r)^{2/3} = 2\sigma^2 \left(\frac{r}{\lambda}\right)^{2/3}, & r \ll \lambda \\ 2\sigma^2, & r \gg \lambda \end{cases},$$

and C_K is a universal constant. From (35) it follows that, in the limit $r \gg \lambda$, formula (34) reduces to (6). In Cartesian reference frame the drift term turns out to be

$$(36) \quad a_i = \left(-\frac{u_{\parallel}}{\tau(r)} + \gamma \frac{u_{\parallel}^2}{r} + \frac{1}{2} \frac{u_{\perp}^2}{r} + \rho \frac{u_{\parallel} u_{\perp}}{r} \right) \frac{r_i}{r} + \frac{u_{\parallel} u_i}{r}.$$

To ensure the incompressibility in stochastic models the identity $\langle a_i \rangle = 0$ must hold [11], and then since in homogeneous, stationary and isotropic turbulence

$$(37) \quad \langle u_i u_j \rangle = \left[\langle u_{\parallel}^2 \rangle - \frac{1}{2} \langle u_{\perp}^2 \rangle \right] \frac{r_i r_j}{r^2} + \frac{1}{2} \langle u_{\perp}^2 \rangle \delta_{ij},$$

and in the inertial range $\langle u_{\parallel} \rangle = 0$, $\langle u_{\parallel} u_{\perp} \rangle = 0$ and $\langle u_{\perp}^2 \rangle = \frac{8}{3} \langle u_{\parallel}^2 \rangle$, it follows that $\gamma = -7/3$.

The parameter ρ is determined by imposing the consistency with some other Eulerian statistical moments, as in the Moments Approximation approach [11]. Multiplying equation (29) by $u_{\parallel}^k u_{\perp}^n$ and integrating with respect to $2\pi u_{\perp} du_{\parallel} du_{\perp}$ yields

$$(38) \quad \begin{aligned} & \frac{2}{r} m_{k+1,n} + \frac{\partial}{\partial r} m_{k+1,n} + \frac{k}{\tau} m_{k,n} \\ & + \frac{4}{3} \frac{k}{r} m_{k+1,n} - \frac{3}{2} \frac{k}{r} m_{k-1,n+2} - \rho \frac{k}{r} m_{k,n+1} = \\ & C_0 \varepsilon \{ k(k-1) m_{k-2,n} + n^2 m_{k,n-2} \}, \end{aligned}$$

where $m_{k,n} = \langle u_{\parallel}^k u_{\perp}^n \rangle = C_{k,n} (\varepsilon r)^{2/3}$. Equation (38) gives a relationship among all the Eulerian statistics of the Markov model (36). In particular, with $\{k=3, n=0\}$ and $\{k=3, n=0\}$ Eq. (38) gives

$$(39) \quad \rho = \frac{1}{m_{3,1}} \left[2m_{4,0} + \frac{r}{3} \frac{\partial m_{4,0}}{\partial r} + C_0 \varepsilon r \frac{m_{3,0}}{m_{2,0}} - \frac{3}{2} m_{2,2} \right].$$

Using DNS data to compute the Eulerian statistics $m_{k,n}$ needed to obtain ρ , in Ref. [5] ρ has been estimated as $\rho = -3653/651 \sim -5.6$.

4. Numerical simulations.

4.1. Determination of scales

It is well-known that a large number of scales occurs in turbulent flows, in particular in the ocean these vary for amplitude, depth and other parameters related to the considered domain. Since the stream function (7) is referred to the Gulf Stream, it can be stated

$$(40) \quad \sigma^2 = 7.47 \text{ km}^2 \text{ d}^{-2}, \quad \tau_L = 1 \text{ d},$$

where the length and time physical dimension are expressed in Kilometers (km) and days (d), respectively. Remembering the definition of τ_L (6) and the corresponding definition of λ from first line in (35), i.e. $\lambda = \varepsilon^{-1}(2\sigma^2/C_K)^{3/2}$, the other scales of the process are determined as

$$(41) \quad \varepsilon = 2.49 \text{ km}^2 \text{ d}^{-3}, \quad \lambda = 8.19 \text{ km},$$

where $C_0 = 6$ and $C_K = 2$ are assumed.

Numerical simulations of the Lagrangian stochastic model introduced in §3 are largely performed and discussed in [15]. Here a selection of them is presented. Two cases with the same stream function (7), which differ for the scale factor ψ_0 , are analyzed:

- case A: $\psi_0 = 4000 \text{ km}^2 \text{ d}^{-1} \Rightarrow s_c = 100 \text{ km d}^{-1}$,
- case B: $\psi_0 = 8000 \text{ km}^2 \text{ d}^{-1} \Rightarrow s_c = 200 \text{ km d}^{-1}$.

The numerical simulations performed and parameter values are summarized in Table 1.

Let \mathcal{L} be the lengthscale of the gradient of U , it can be estimated dividing the modulus of \mathbf{U} by the maximum of ψ_{yy} :

- case A: $[\psi_{yy}]_{max} \simeq 2 \text{ d}^{-1}$ for $y \simeq 25 \text{ km}$

$$\Rightarrow \mathcal{L} = \frac{|\mathbf{U}|}{[\psi_{yy}]_{max}} \simeq 25 \text{ km} \quad \text{when } |\mathbf{U}| \simeq 50 \text{ km d}^{-1},$$

- case B: $[\psi_{yy}]_{max} \simeq 4 \text{ d}^{-1}$ for $y \simeq 25 \text{ km}$

$$\Rightarrow \mathcal{L} = \frac{|\mathbf{U}|}{[\psi_{yy}]_{max}} \simeq 25 \text{ km} \quad \text{when } |\mathbf{U}| \simeq 100 \text{ km d}^{-1}.$$

From these estimations it follows that the Eulerian lengthscale λ and the average velocity gradient lengthscale \mathcal{L} are such as the inhomogeneity of the field \mathbf{U} becomes important when $r > \lambda$. This justify the application

of the Lagrangian stochastic model described in §3.3 for particle relative dispersion.

It is well-known that the kinematic viscosity of water is $\nu = 10^{-2} \text{ cm}^2 \text{ s}^{-1} = 8.64 \cdot 10^{-8} \text{ km}^2 \text{ d}^{-1}$, then with ν and ε it possible to estimate Kolmogorov scales as follows:

$$\begin{aligned}\eta &\equiv (\nu^3/\varepsilon)^{1/4} = 4 \cdot 10^{-6} \text{ km} = 0.4 \text{ cm}, \\ u_\eta &\equiv (\varepsilon\nu)^{1/4} = 2.15 \cdot 10^{-2} \text{ km d}^{-1} = 2.49 \cdot 10^{-2} \text{ cm s}^{-1}, \\ \tau_\eta &\equiv (\nu/\varepsilon)^{1/2} = 1.86 \cdot 10^{-4} \text{ d} \simeq 16 \text{ s}.\end{aligned}$$

When the Kolmogorov lengthscale η and the Eulerian lengthscale λ are known, the Reynolds number of process under consideration can be estimated. In fact, from definition $\mathcal{R}e = \sigma\lambda/\nu$, it turns out that $\lambda/\eta = \mathcal{R}e^{3/4}$ and then for the present case $\mathcal{R}e = 2.6 \cdot 10^8$, which is in agreement with $\mathcal{R}e$ for ocean turbulence.

Table 1. List of simulated cases and parameter values.

label	(x_0, y_0) (km)	N part.	Δt (d)	σ^2 ($\text{km}^2 \text{d}^{-2}$)	ε ($\text{km}^2 \text{d}^{-3}$)	C_0	C_K
A1	(0,50)						
A2	(0,0)						
A3	$ \mathbf{U} = \mathbf{U} (\text{B2})$	400	$3 \cdot 10^{-5}$	7.47	2.49	6	2
B1	(0,50)						
B2	(0,0)						

4.2. Numerical results

4.2.1. Case A1

The oscillating motion of the meandering jet, see Fig. 4.2.1(a), causes oscillations also to the enlarging of the oil spill, see Figs. 4.2.1(b,c,d). In particular, the two maxima in Fig. 4.2.1(d) at $t \simeq 6 \text{ d}$ and $t \simeq 8 \text{ d}$ correspond to the maximum of ψ_{yy} , see Fig. 4.2.1, in $(x \simeq 500 \text{ km}, y \in [-50, 0] \text{ km})$ and $(x \simeq 700 \text{ km}, y \in [0, +50] \text{ km})$, respectively. Finally, at $t \simeq 9 \text{ d}$ the oil spill is moving in a zone where the gradient of U is maximum and than it is going towards a zone with $\psi_{yy} \simeq 0$, which explains the decreasing of the curve in Fig. 4.2.1(d).

The curve plotted in Fig. 4.2.1(c) shows maxima and minima in phase opposition with respect to Fig. 4.2.1(d). This fact can be proved analytically by calculation of gradient of U in x where derivatives of $A \cos(kx)$ and $k^2 A^2 \sin^2(kx)$ appear.

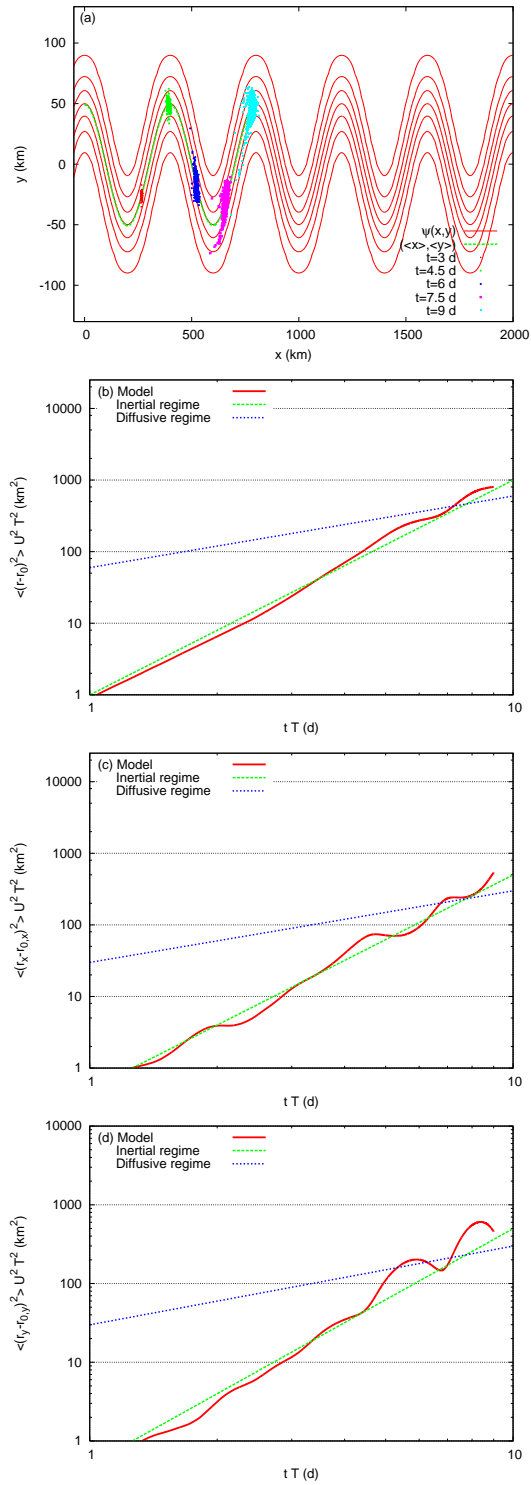


Fig. 1. Case A1: (a) centre of mass trajectory and particles positions at five different instants, (b) relative separation variance, (c) relative separation variance in x -direction, (d) relative separation variance in y -direction.

4.2.2. Case A2

Looking to the meandering of stream function in Fig. 4.2.2(a), the enlarging of the oil spill in the y -direction is reducing when particles approach the minimum around $x \simeq 200$ m. In fact, in the plot shown in Fig. 4.2.2(d) a minimum appears at $t \simeq 6$ d. However, at $t \simeq 7.5$ d the number of uncorrelated particles is so large that, since some of them are moving towards North, the enlarging of the oil spill in the y -direction strongly increases.

4.2.3. Case B1

Looking at Fig. 4.2.3(a), a larger advection velocity than in the case A spreads the oil spill along the meandering jet more than in the case A, see Fig. 4.2.1. This fact can be re-view in the faster oscillating motion shown in Fig. 4.2.3(d) with respect to Fig. 4.2.1(d). The stronger average velocity field advects particles through an higher number of tops and bottoms of the meandering jet. The explanation of maxima and minima which relates Figs. 4.2.3(a,d) is the same as for Figs. 4.2.1(a,d).

4.2.4. Case B2

The curve plotted in Fig. 4.2.4(d) shown a maximum at $\tilde{t} \simeq 7$ d and a minimum at $\tilde{t} \simeq 8.5$ d, which have correspondence in Fig. 4.2.4(a) in $(x \simeq 250 \text{ km}, y \simeq -70 \text{ km})$, where ψ_{yy} is maximum, and $(\tilde{x} \simeq 300 \text{ km}, y \simeq -50 \text{ km})$, where $\psi_{yy} \simeq 0$, respectively.

4.3. Case A3

This case consider a release in the average velocity field labeled A in a source point such that the initial value of $|\mathbf{U}|$ is the same as in the case B2. The aim of this simulation is to study the differences due to different velocity gradient. In particular the gradient of case A is one half the gradient of case B. Comparing plots of A3 and B2 several analogies appear in the motion of centre of mass, in the enlarging of the oil spill and in the curves of particle separation variances. In particular, looking to Figs. 4.3(b) and 4.2.4(b), the separation variance of case A3 turns out to be one half than in the case A, as it was expected. However, only the x -component of separation variance emerges to be halved, see Figs. 4.3(c) and 4.2.4(c). For what concern separation in y -direction, it occurs a weak delay that shifts forward maxima and minima, which are decreased around 20% except at $t = 9$ d that is strongly lower, see Figs. 4.3(d) and 4.2.4(d).

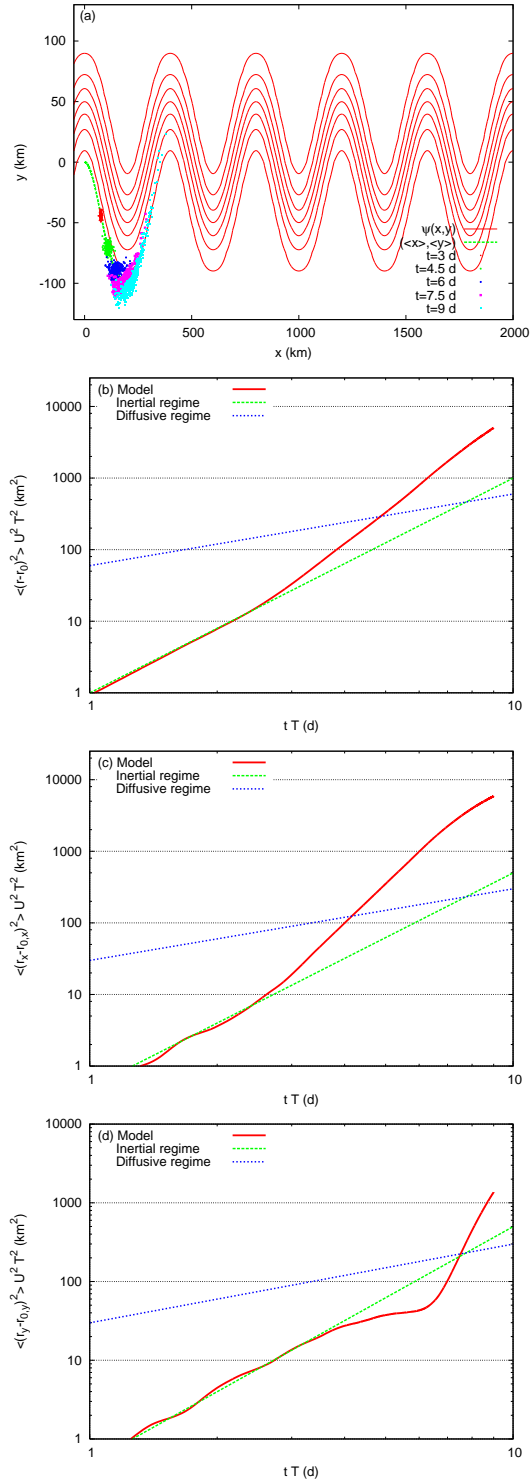


Fig. 2. Case A2: the same as in Fig. 4.2.1

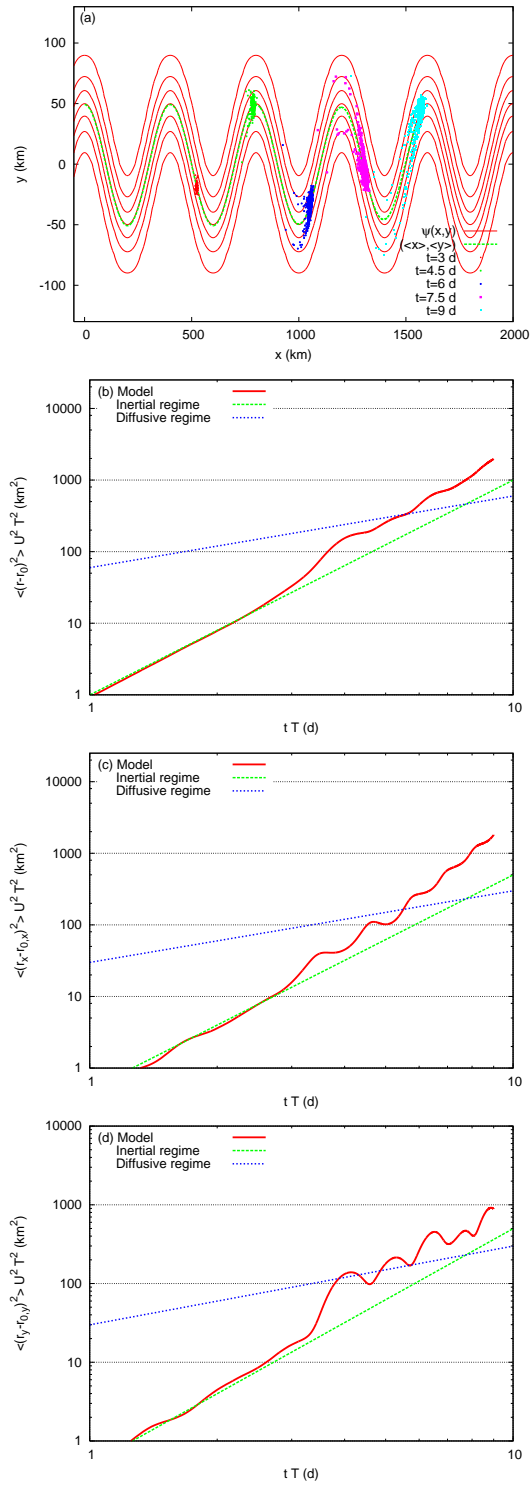


Fig. 3. Case B1: the same as in Fig. 4.2.1

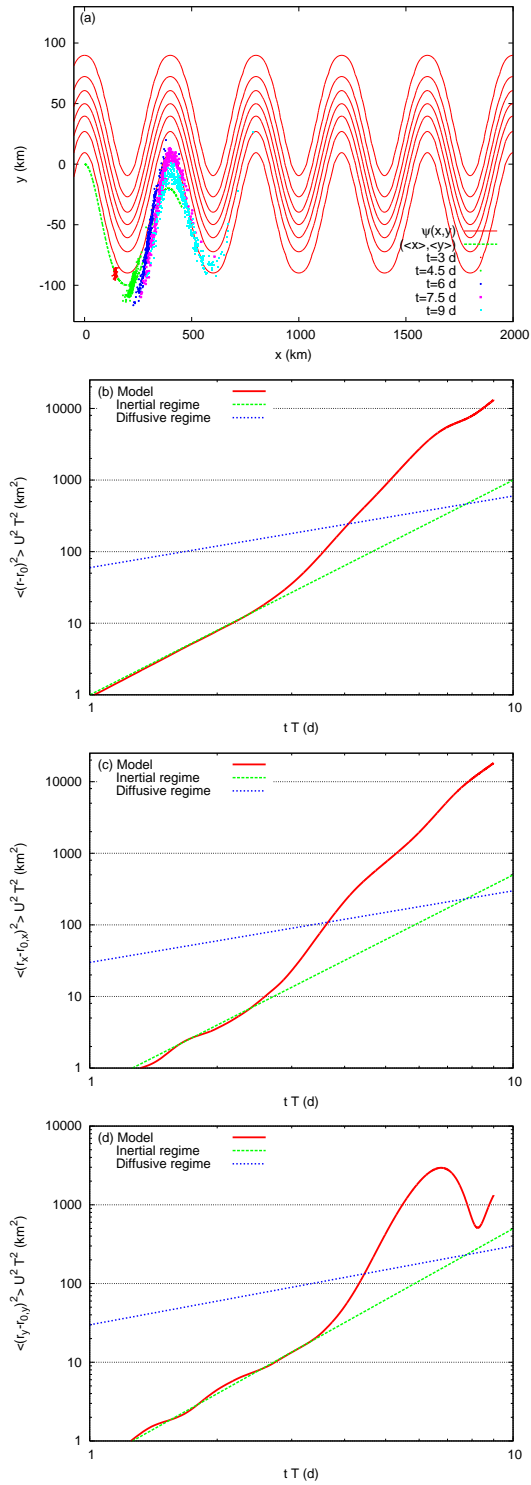


Fig. 4. Case B2: the same as in Fig. 4.2.1

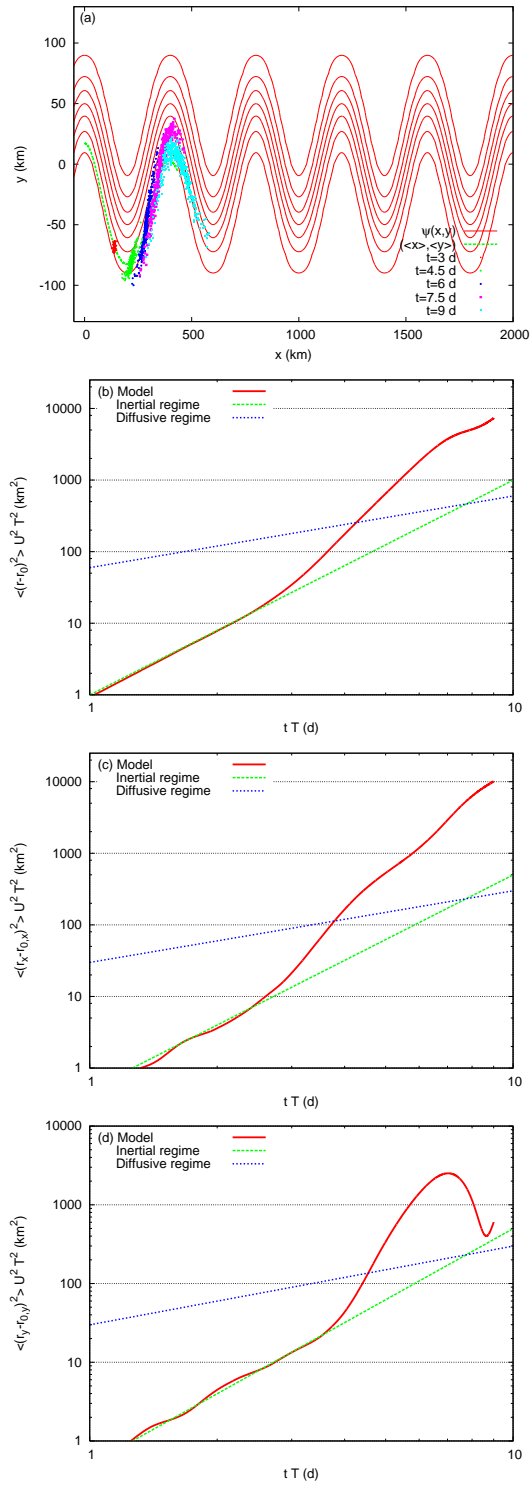


Fig. 5. Case A3: the same as in Fig. 4.2.1

5. Conclusion.

A Lagrangian stochastic model to simulate turbulent dispersion of oil spills on ocean surface is formulated. The oil spills are assumed as non-reacting passive tracers. The model includes both large and small scale turbulence. Large scale motion, which drives the centre of mass, is assumed in the analytical form proposed by A.S. Bower for meandering jet in the Gulf Stream [4]. Small scale motion is constructed assuming homogeneous, stationary and isotropic turbulence, independent of the large scale motion, for particle separation less than both the Eulerian and the average velocity gradient lengthscales. In this range particles are correlated and the Lagrangian stochastic process developed in Ref. [5] is adopted. When particle separation is larger than Eulerian lengthscales, such that the motion of particle is statistically independent and the large scale average velocity field is not negligible, particle trajectories are simulated by the sum of the average velocity field and an Ornstein–Uhlenbeck stochastic process.

Two case studies are considered which differ in respect of the maximum velocity. The ‘faster’ field stronger advects the centre of mass as well as it generates a larger particle separation variance as a consequence of an higher velocity gradient.

Comparison between releases from the centre and the boundary of the meandering jet are also done. In the first case it emerges that when particles are independent they spread around the centre of mass but travelling to zone that obligatory have a less velocity intensity, as a consequence a tail of tracers delayed is build. On the contrary, in the second case, particles are dispersed both forward and backward to the centre of mass and then the trajectory is splitted between a faster part, towards North, and a slower part towards South, generating a stirring North-East South-West of the oil spill. Comparing both releases for the same velocity field, an higher particle separation variance occurs for boundary releases and this can be due to the different intensity of the velocity gradient in different zones.

The work done suggests for further development the quantitative analysis of the relationship between the gradient of the large scale velocity field and the small scale transverse particle separation variance. Moreover, a similar analysis can be performed for a stream function ables to reproduce a large scale velocity field with recirculation.

REFERENCES

1. J. M. Redondo and A. K. Platonov, Self-similar distribution of oil spills in European coastal waters, *Environ. Res. Lett.*, vol. 4, p. 014008 (10pp), 2009.

2. A. K. Luhar, M. F. Hibberd, and P. J. Hurley, Comparison of closure schemes used to specify the velocity PDF in Lagrangian stochastic dispersion models for convective conditions, *Atmos. Environ.*, vol. 30, pp. 1407–1418, 1996.
3. M. Veneziani, A. Griffa, A. M. Reynolds, and A. J. Mariano, Oceanic turbulence and stochastic models from subsurface Lagrangian data for the Northwest Atlantic Ocean, *J. Phys. Oceanogr.*, vol. 34, pp. 1884–1906, 2004.
4. A. S. Bower, A simple kinematic mechanism for mixing fluid parcels across a meandering jet, *J. Phys. Oceanogr.*, vol. 21, pp. 173–180, 1991.
5. G. Pagnini, Lagrangian stochastic models for turbulent relative dispersion based on particle pair rotation, *J. Fluid Mech.*, vol. 616, pp. 357–395, 2008.
6. A. S. Monin and R. V. Ozmidov, *Turbulence in the Ocean*. Dordrecht: Reidel, 1985.
7. A. E. Gargett, Ocean turbulence, *Ann. Rev. Fluid Mech.*, vol. 21, pp. 419–451, 1989.
8. A. S. Monin and A. M. Yaglom, *Statistical Fluid Mechanics*, vol. I. Cambridge: MIT Press, 1971.
9. D. Thomson, Criteria for the selection of stochastic models of particle trajectories in turbulent flows, *J. Fluid Mech.*, vol. 180, pp. 529–556, 1987.
10. D. Thomson, A stochastic model for the motion of particle pairs in isotropic high-Reynolds-number turbulence, and its application to the problem of concentration variance, *J. Fluid Mech.*, vol. 210, pp. 113–153, 1990.
11. G. Pedrizzetti and E. A. Novikov, On Markov modelling of turbulence, *J. Fluid Mech.*, vol. 280, pp. 69–93, 1994.
12. O. A. Kurbanmuradov, Stochastic Lagrangian models for two-particle relative dispersion in high-Reynolds number turbulence, *Monte Carlo Methods and Appl.*, vol. 3, no. 1, pp. 37–52, 1997.
13. M. S. Borgas and P. K. Yeung, Relative dispersion in isotropic turbulence. Part 2. A new stochastic model with Reynolds-number dependence, *J. Fluid Mech.*, vol. 503, pp. 125–160, 2004.
14. H. Risken, *The Fokker-Planck Equation. Methods of Solution and Applications*. Springer-Verlag, second ed., 1989.
15. S. Strada, *Turbulent Dispersion of Passive Tracers on Sea Surface*. Master thesis, Dept. Physics, University of Bologna, 2007. In Italian.